



University
of Glasgow | School of
Computing Science

Algorithm Selection for Maximum Common Subgraph

Paulius Dilkas

School of Computing Science
Sir Alwyn Williams Building
University of Glasgow
G12 8QQ

Level 4 Project — 14th December 2017

Education Use Consent

I hereby give my permission for this project to be shown to other University of Glasgow students and to be distributed in an electronic format. **Please note that you are under no obligation to sign this declaration, but doing so would help future students.**

Name: _____ Signature: _____

Contents

1	Introduction	1
1.1	The Algorithms	2
2	Problem Instances	3
2.1	Labelled Graphs	3
2.1.1	Characteristics of Graph Labelling	3
2.2	Unlabelled Graphs	4
3	Generating Data	6
3.1	Running Time of Algorithms	6
3.1.1	Unlabelled Graphs	7
3.1.2	Vertex-Labelled Graphs	9
3.1.3	Vertex- and Edge-Labelled Graphs	9
3.2	Graph Features	9
3.2.1	Distributions of Features	10
4	Machine Learning Models & Their Evaluation	18
4.1	Unlabelled Graphs	20
4.1.1	Error Rates	20
4.1.2	Variable Importance	21
4.1.3	Margins	24
4.1.4	Partial Dependence	24
4.1.5	Runtime Comparison	26
4.2	Vertex-Labelled Graphs	27

4.3	Vertex- and Edge-Labelled Graphs	27
-----	--	----

Chapter 1

Introduction

We start with a definition of graphs suitable for the empirical data described in Chapter 2 and used in Chapter 3.

Definition 1.0.1. Let S be a set and let k be a non-negative integer. Then $[S]^k$ denotes the set of k -subsets of S [33], i.e.,

$$[S]^k = \{A \subseteq S : |A| = k\}.$$

Definition 1.0.2. An *undirected multigraph* is a pair (V, E) , where V is a set of vertices and E is a set of edges, together with a map $E \rightarrow V \cup [V]^2$, which assigns one or two vertices to each edge [6]. If an edge is assigned to a single vertex, it is called a *loop*. When several edges map to the same pair of vertices, they are referred to as *multiple edges*.

We formulate all of the definitions in terms of undirected multigraphs as some of the graphs in Chapter 2 contain multiple edges and many contain at least one loop. In the rest of the dissertation, we will refer to undirected multigraphs simply as graphs. Next we adapt some basic graph theory definitions to work with our definition of a multigraph.

Definition 1.0.3. Two graphs $G_1 = (V_1, E_1)$ and $G_2 = (V_2, E_2)$ are said to be *isomorphic* if there is a bijection $f: V_1 \rightarrow V_2$ such that for all $v \in V_1 \cup [V_1]^2$, the number of edges in E_1 that are mapped to v is equal to the number of edges in E_2 that are mapped to $f(v)$, where $f(v) = \{f(v_1), f(v_2)\}$ if $v = \{v_1, v_2\} \in [V_1]^2$ [26].

Definition 1.0.4. A graph $G_2 = (V_2, E_2)$ is a *subgraph* of graph $G_1 = (V_1, E_1)$ if $V_2 \subseteq V_1$ and $E_2 \subseteq E_1$ [6].

Definition 1.0.5. An *induced subgraph* of a graph $G = (V, E)$ is a graph $H = (S, E')$, where $S \subseteq V$ is a set of vertices and $E' \subseteq E$ is a set of edges that are mapped to $S \cup [S]^2$ [26].

Definition 1.0.6. A *clique* C in a graph $G = (V, E)$ is a subset of V such that $\forall v_1, v_2 \in C$ with $v_1 \neq v_2$, there is an edge in E mapping to $\{v_1, v_2\}$ [24].

Finally, we define the main problem dealt with in this project.

Definition 1.0.7. A *maximum common (induced) subgraph* between graphs G_1 and G_2 is a graph $G_3 = (V_3, E_3)$ such that G_3 is isomorphic to induced subgraphs of both G_1 and G_2 with $|V_3|$ maximised [26]. The *maximum common (induced) subgraph problem* is the problem of finding a maximum common subgraph between two given graphs $G_1 = (V_1, E_1)$ and $G_2 = (V_2, E_2)$, usually expressed as a bijection between two subsets of vertices $U_1 \subseteq V_1$ and $U_2 \subseteq V_2$.

The purpose of this project is to create and explore machine-learning-based algorithm *portfolios*, i.e., machine learning models whose main goal is to provide a mapping, assigning the best-performing algorithm to each problem instance [2, 27].

1.1 The Algorithms

We consider four algorithms that were shown to be competitive in a paper by McCreesh *et al.* [23]: $k \downarrow$ [9], MCSPLIT, MCSPLIT \downarrow [23], and the clique encoding [20]. The way some of these algorithms work relates to two other problems: the maximum clique problem and the subgraph isomorphism problem, both defined as follows:

Definition 1.1.1. Given a graph G , the *maximum clique problem* is an optimisation problem asking for a clique in G with maximum cardinality [24].

Definition 1.1.2. Given two (finite) graphs G_1 and G_2 , the *subgraph isomorphism problem* is the decision problem of determining whether G_1 is isomorphic to a subgraph of G_2 [4].

$k \downarrow$ algorithm [9] starts by trying to solve the subgraph isomorphism problem, i.e. finding the pattern graph in the target graph. If that fails, it allows a single vertex of the pattern graph to not match any of the target graph vertices and tries again, allowing smaller and smaller pattern graphs until it finds a solution. The number of vertices of the pattern graph that are allowed this additional freedom is represented by k . More specifically, the algorithm creates a domain for each pattern graph vertex, which initially includes all vertices of the target graph and k wildcards. The domains are filtered with various propagation techniques. Then the search begins with a smallest domain (not counting wildcards), a value is chosen, and domains are filtered again to eliminate the chosen value.

The clique encoding [20] solves the maximum common subgraph problem by creating a new (association) graph and transforming the problem into an instance of the maximum clique problem [16], which is then solved by a sequential version of the maximum clique solver by McCreesh and Prosser [21], which is a branch and bound algorithm that uses bitsets and greedy colouring. Colouring is used to provide a quick upper bound: if a subgraph can be coloured with k colours, then it cannot have a clique of size more than k .

MCSPLIT [23] is a branch and bound algorithm that builds its own bit string labels for vertices in both pattern and target graphs. Once it chooses to match a vertex u in graph G_1 with a vertex v in graph G_2 , it iterates over all unmatched vertices in both graphs, adding a 1 to their labels if they are adjacent to u or v and 0 otherwise. That way a vertex can only be matched with vertices that have the same labels. The labels are also used in the upper bound heuristic function using the rule that if a particular label is assigned to m vertices in G_1 and n vertices in G_2 , then up to $\min\{m, n\}$ pairs can be matched for that label.

MCSPLIT \downarrow is a variant of MCSPLIT mentioned but not explained in the original paper [23]. It is meant to be similar to $k \downarrow$ in that it starts by trying to find a subgraph isomorphism and keeps decreasing the size of common subgraphs that it is interested in until a solution is found. Based on the source code¹, there are a few key differences between MCSPLIT \downarrow and MCSPLIT:

- Instead of always looking for larger and larger common subgraphs, we have a goal size and exit early if a common subgraph of that size is found.
- The goal size is decreased if the search finishes without a solution.
- Having a big goal size allows the heuristic to be more selective and prune more of the search tree branches.

¹<https://github.com/jamestrimble/ijcai2017-partitioning-common-subgraph/blob/master/code/james-cpp/mcsp.c>

Chapter 2

Problem Instances

We use two graph databases that contain a large variety of graphs differing in size, various characteristics, and the way they were generated. The MCSPLIT paper [23] used the same data to compare these (and a few constraint programming) algorithms and found MCSPLIT to win with unlabelled graphs described in Section 2.1 of this paper, the clique encoding to win with labelled graphs, and MCSPLIT \downarrow to win with unlabelled graphs from Section 2.2. However, in some cases the difference in performance between MCSPLIT and the clique encoding or between MCSPLIT \downarrow and $k \downarrow$ was very small.

2.1 Labelled Graphs

All of the labelled graphs are taken from the ARG Database [8, 29], which is a large collection of graphs for benchmarking various graph-matching algorithms. The graphs are generated using several algorithms:

- randomly generated,
- 2D, 3D, and 4D meshes,
- and bounded valence graphs.

Furthermore, each algorithm is executed with several (3–5) different parameter values. The database includes 81400 pairs of labelled graphs. Their unlabelled versions are used as well.

2.1.1 Characteristics of Graph Labelling

For the purposes of this paper, we look at two types of labelled graphs: those that have their vertices labelled and those that have both vertices and edges labelled. We define them as follows (the definitions are loosely inspired by [1]):

Definition 2.1.1. A graph $G = (V, E)$ is a *(vertex) labelled graph* if it has an associated vertex labelling function $\mu: V \rightarrow \{0, \dots, N - 1\}$ for some $N \in \{2, \dots, |V|\}$.

Definition 2.1.2. A graph $G = (V, E)$ is a *fully labelled graph* if it is a vertex labelled graph and it has an associated edge labelling function $\zeta: E \rightarrow \{0, \dots, M - 1\}$ for some $M \in \{2, \dots, |E|\}$.

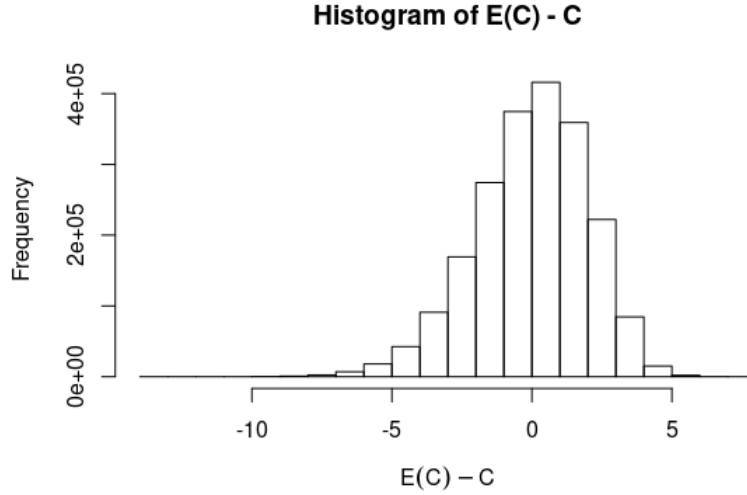


Figure 2.1: Histogram of the difference between the expected number of vertices assigned each label and the actual number (for all labelled graphs)

Specifically, note that:

- If a graph is labelled, then all its vertices (and possibly edges) are assigned a label.
- We are only considering finite sets of labels, represented by non-negative integers.

Now we need a way to choose N and M . For that we formally define how labelling is implemented in the ARG database:

Definition 2.1.3. A graph $G = (V, E)$ is said to have a $p\%$ (*vertex*) *labelling* if

$$N = \max \left\{ 2^n : n \in \mathbb{N}, 2^n < \left\lfloor \frac{p}{100\%} \times |V| \right\rfloor \right\}.$$

The default value for p is 33%.

The publications associated with the database [8, 29] say nothing about how the labels are distributed among the N values. We calculate the number of vertices that were assigned each label for each graph (represented by C) and compare those values with the numbers we would expect from a uniform distribution (represented by $E(C)$). We plot a histogram of the difference $E(C) - C$ in Figure 2.1 and observe that the difference is normally distributed around 0.

2.2 Unlabelled Graphs

We also include a collection of benchmark instances for the subgraph isomorphism problem¹ (with the biochemical reactions dataset excluded since we are not dealing with directed graphs). It contains only unlabelled graphs and consists of the following sets:

¹<http://liris.cnrs.fr/csolnon/SIP.html>

images-CVIU11 Graphs generated from segmented images. 43 pattern graphs and 146 target graphs, giving a total of 6278 instances.

meshes-CVIU11 Graphs generated from meshes modelling 3D objects. 6 pattern graphs and 503 target graphs, giving a total of 3018 instances. Both `images-CVIU11` and `meshes-CVIU11` datasets are described in [5].

images-PR15 Graphs generated from segmented images [31]. 24 pattern graphs and a single target graph, giving 24 instances.

LV Graphs with various properties (connected, biconnected, triconnected, bipartite, planar, etc.). 49 graphs are paired up in all possible ways, giving $49^2 = 2401$ instances.

scalefree Scale-free networks generated using a power law distribution of degrees (100 instances).

si Bounded valence graphs, 4D meshes, and randomly generated graphs (1170 instances). This is the unlabelled part of the ARG database. `LV`, `scalefree`, and `si` datasets are described in [30, 35].

phase Random graphs generated to be close to the satisfiable-unsatisfiable phase transition (200 instances) [22].

largerGraphs Larger instances of the `LV` dataset. There are 70 graphs, giving $70^2 = 4900$ instances. The separation was made and used in [9, 15, 23].

Remark 2.2.1. This set of instances was taken from the repository² for the MCSPLIT paper [23] and has some minor differences from the version on Christine Solnon’s website.

Remark 2.2.2. Since $k \downarrow$ comes from the subgraph isomorphism problem background, it treats the two (pattern and target) graphs differently. Therefore, when graphs are not divided into patterns and targets, we run the algorithms with both orders $((G_1, G_2)$ and $(G_2, G_1))$.

²<https://github.com/jamestrimble/ijcai2017-partitioning-common-subgraph>

Chapter 3

Generating Data

A machine learning (ML) model requires data to learn from. We are using an R package called LLAMA [12, 13], which helps to train and evaluate ML models in order to compare algorithms and was used to create algorithm portfolios for the travelling salesperson problem [14] and the subgraph isomorphism problem [15]. First, we run each algorithm on all pairs of pattern-target graphs and record the running times (described in Section 3.1). Then, we adapt a graph feature extractor program used in [15] to handle the binary format of the ARG Database [8, 29], run it on all graphs, and record the features in a way described in Section 3.2.

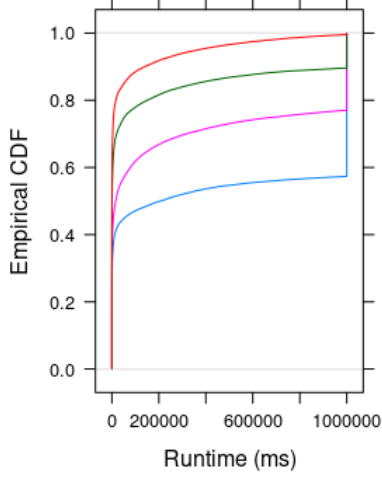
3.1 Running Time of Algorithms

The algorithms were compiled with gcc 6.3.0 and run on Intel Xeon E5-2697A v4 (2.60 GHz) processors with a 1000 s time limit. A Makefile was created to run multiple experiments in parallel with, e.g., `make -j 64`, which generates pairs of graph filenames for all datasets, runs the selected algorithms with various command line arguments, redirects their output to files that are later parsed using `sed` and regular expressions into the CSV format. For each algorithm, we keep the full names of pattern and target graphs, the number of vertices in the returned maximum common subgraph, running time as reported by the algorithms themselves, and the number of explored nodes in the search tree. Entries with running time greater than or equal to the timeout value are considered to have timed out. The aforementioned node counts are collected but not currently used. Afterwards, the answers of different algorithms are checked for equality (for algorithms that did not time out).

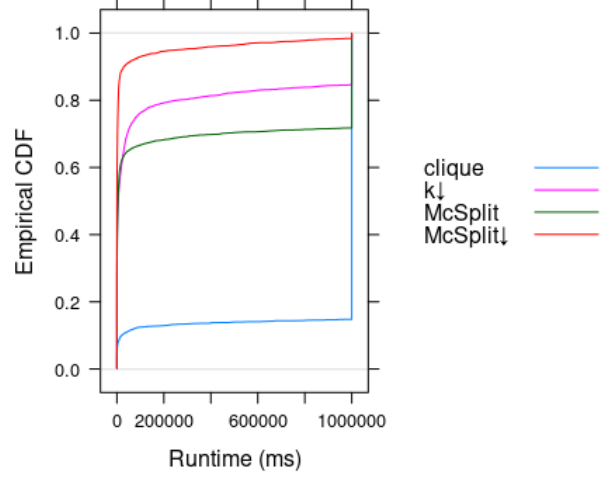
Some limitations had to be enforced to avoid running out of memory. First, the clique algorithm requires $O(n^2m^2)$ memory for a pair of graphs with n and m vertices [9, 20], so its virtual memory usage was limited to 7 GB with `ulimit -v` and the instances from Section 2.2 (which contain much larger graphs) were restricted to $m \times n < 16,000$. Second, having almost 10^5 problem instances and analysing 7 different kinds of labelling (according to Definition 2.1.3) results in too much data for the ML algorithm. Therefore, we sample 30,000 out of 81,400 instances from Section 2.1. The sample is drawn once and used for training ML models for both types of labelling (vertex labels and both vertex and edge labels). As with 50% labelling most instances are solved within the time limit, sampling from the whole database still leaves us with enough relevant data.

`k ↓` was further modified to accept graphs with vertex labels by adding an additional constraint for matching labels on line 8 of the `klessSubgraphIsomorphism` function [9]. Likewise, different implementations of the clique algorithm were combined to support both the binary format of the ARG Database and the plaintext format of Section 2.2.

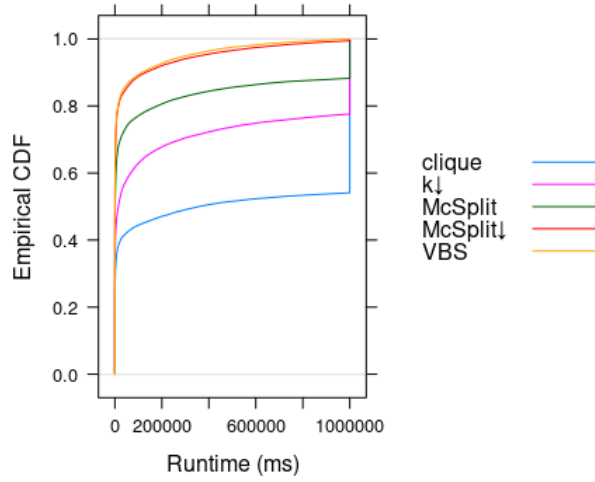
In the rest of this section we explore and compare how the algorithms performed on the three different



(a) Data from Section 2.1, the ARG Database



(b) Data from Section 2.2



(c) All unlabelled data

Figure 3.1: Comparison of the runtimes of algorithms on unlabelled data

subproblems under consideration, those of having no labels, vertex labels, and both vertex and edge labels. We introduce *empirical cumulative distribution function (ECDF)* plots [34]: for each unit of time on the horizontal axis, the value on the vertical axis represents what part of the problem instances was solved in that amount of time or less.

3.1.1 Unlabelled Graphs

We plot the ECDF plots for unlabelled graphs in both databases in Figure 3.1. We can check that the orderings of the algorithms in parts (a) and (b) of Figure 3.1 are the same as in Figures 3a and 4 in the MCSPLIT paper [23]. Namely, MCSPLIT outperforms $k \downarrow$ in Figure 3.1a, and the opposite happens in Figure 3.1b. In Figure 3.1c we also plot a curve for the *virtual best solver (VBS)*, i.e., a perfect algorithm portfolio that always chooses the best-performing algorithm for each problem instance. Note that the difference between MCSPLIT \downarrow and VBS is very small. Therefore, a portfolio cannot provide significant performance benefits for this subproblem. We also provide a heatmap in Figure 3.2 to compare the runtimes of the algorithms on a per-instance basis.

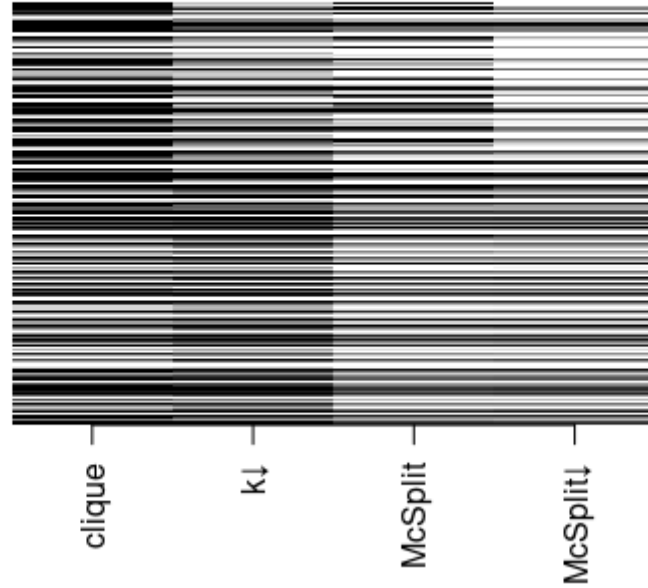


Figure 3.2: A heatmap of \log_{10} runtimes: light colours for low running times and black for timing out

Remark 3.1.1. Not every problem instance gets a line of pixels on the heatmap. Therefore, the column for the clique encoding may look darker than it actually is. Furthermore, there are problem instances where $k \downarrow$ performs better than the other algorithms, even though it may not be apparent from the heatmap.

Table 3.1 shows that most of the datasets have multiple algorithms that managed to outperform the others for some problem instances. Thus, looking at the differences between different datasets will not be enough to predict the best algorithm.

Remark 3.1.2. More specifically, Table 3.1 shows the numbers of times that each algorithm's runtime was lower than or equal to the runtimes of other algorithms. Therefore, if 2 or more lowest runtimes are equal (as can often happen with single-digit runtimes), both algorithms are marked as winning in the table.

Given this information, we would expect the ML algorithm to suggest using MCSPLIT and MCSPLIT \downarrow most

Dataset	clique	$k \downarrow$	MCSPLIT	MCSPLIT \downarrow
images-CVIU11	0	32	79	1081
images-PR15	0	0	0	24
largerGraphs	0	14	30	167
LV	90	30	489	439
meshes-CVIU11	0	13	0	23
phase	0	0	0	0
scalefree	0	0	0	80
si	0	10	102	1135
ARG Database	1443	141	21965	27305
Total	1533	240	22665	30254

Table 3.1: The number of times each algorithm was the best, for each dataset

of the time, occasionally consider the clique encoding, and mostly forget about $k \downarrow$.

3.1.2 Vertex-Labelled Graphs

3.1.3 Vertex- and Edge-Labelled Graphs

3.2 Graph Features

The initial set of features is based on the algorithm selection paper for the subgraph isomorphism problem [15] and consists of the following:

1. number of vertices,
2. number of edges,
3. mean degree,
4. maximum degree,
5. density,
6. mean distance between all pairs of vertices,
7. maximum distance between all pairs of vertices,
8. standard deviation of degrees,
9. number of loops,
10. proportion of all vertex pairs that have a distance of at least 2, 3, and 4,
11. whether the graph is connected.

Definition 3.2.1. For a graph G with n vertices and m edges, the (*edge*) *density* is defined to be the proportion of potential edges that G actually has [6]. The standard formula used for simple graphs is

$$\frac{m}{\binom{n}{2}} = \frac{2m}{n(n-1)}.$$

Even though some of our graphs contain multiple edges and loops, we stick to this formula as it was used in [15] and it does not break the ML algorithm in any way to have the theoretical possibility of density greater than 1.

We exclude feature extraction running time as a viable feature by itself since it would not provide any insight into what properties of the graph affect which algorithm is likely to achieve the best performance. Since $k \downarrow$ and MCSPLIT \downarrow both start by looking for (complete) subgraph isomorphisms, they are likely to outperform other algorithms when both graphs are very similar and the maximum common subgraph has (almost) as many vertices as the smaller of the two graphs. Thus, for each feature f in features 1–7 (excluding the rest to avoid division by 0), we also add a feature for the ratio $\frac{f(G_p)}{f(G_t)}$, where G_p and G_t are the pattern and target graphs respectively.

We analyse three different types of labelling and treat them as separate problems: no labels, vertex labels, vertex and edge labels. For the last two types, we add a feature corresponding to p defined in Definition 2.1.3 and collect data for the following values of p : 50%, 33%, 25%, 20%, 15%, 10%, 5%. The values correspond to having about 2, 3, 4, 5, 10, and 20 vertices/edges with the same label on average respectively.

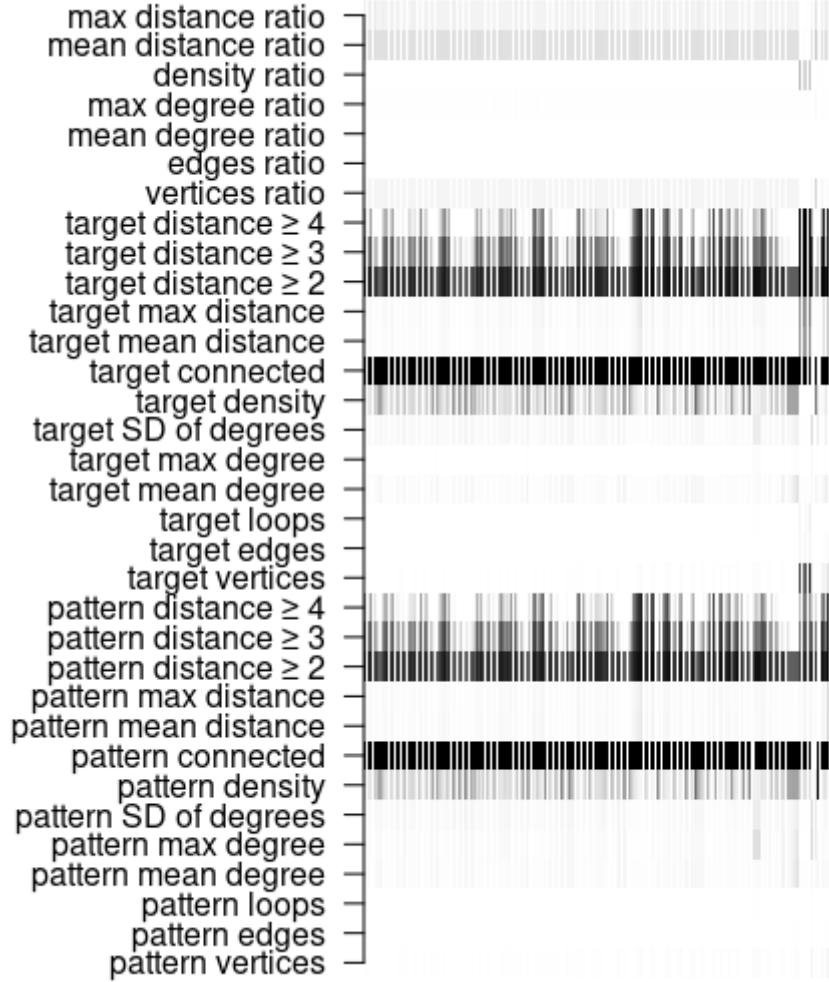


Figure 3.3: A heatmap for normalised features with black denoting the maximum value and white denoting the minimum for each feature

Remark 3.2.1. When working with both vertex and edge labels, we only consider using the same value of p for both vertices and edges. Although this may not be ideal, it reflects how the ARG Database was constructed. Furthermore, there are many ways to label a graph and it is unclear which types of labelling are worth investigating.

3.2.1 Distributions of Features

In this section we plot and discuss how the selected features are distributed in both databases. As the graphs from Section 2.2 contain some very hard instances, we only consider graphs that are part of a pair of graphs solved by at least one algorithm. In order to visualise highly skewed data, we sometimes use density plots. Furthermore, we take log transformations for ratio features. We also plot a heatmap of all features for all of the data in Figure 3.3. The rows that are almost completely white represent features that have several significantly higher values that skew the average.

Firstly, one feature is not plotted as by definition it has only two possible values. 99.81% of graphs from Section 2.1 are connected, compared to 93.19% of graphs from Section 2.2. As both numbers are quite high, they may not be ideal for establishing if connectedness is a significant factor in determining which algorithm performs

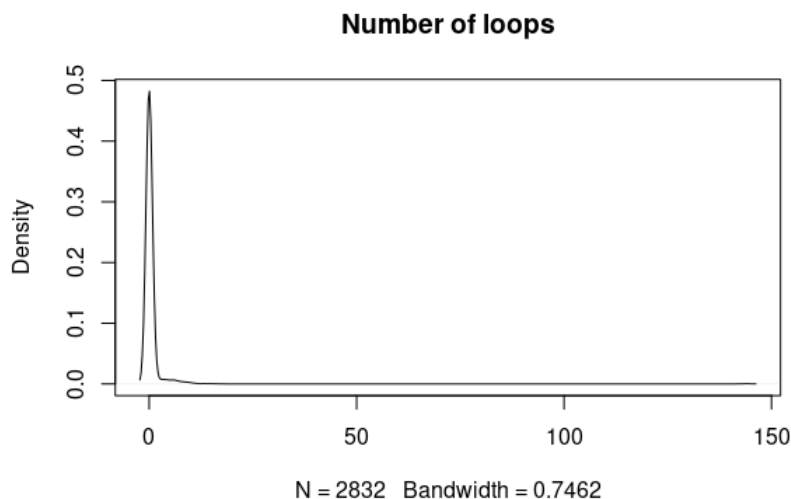


Figure 3.4: Density plot of the number of loops in graphs from Section 2.2

the best. However, many applications in chemistry are only interested in connected graphs [7]. Similarly, the number of loops for graphs from Section 2.1 is not plotted as it varies between two values: 0.98% of the graphs have a single loops, while the remaining majority of graphs have no loops. On the other hand, as shown in Figure 3.4, some (although not many) graphs from Section 2.2 have significantly more loops.

Most of the features for graphs from Section 2.1 are displayed in Figure 3.5. Other than the plot for the number of vertices, which is controlled by the creators of the database, all the other distributions are centred around lower values, with some outliers on the high end. More importantly, we have some graphs that are quite dense and some graphs with higher mean distance values.

The same plots for graphs from Section 2.2 in Figure 3.6 show a similar story, albeit for clearer reasons. Since we filter out graphs that none of the algorithms were able to handle, our sample consists of all of the easy instances and some harder instances that were solved by one or two algorithms. Harder instances typically have more vertices, which means they are also capable of higher values for many other features, hence all of the density plots are right skewed.

Figure 3.7 shows density plots of proportions of pairs of vertices with distance at least k for $k = 2, 3, 4$. For both databases, as k increases, the distributions shift to the left as expected. However, there is one important difference: even with $k = 4$ the plot for graphs from Section 2.2 has its highest peak around 0.9, which means that adding features for $k \geq 5$ could be valuable.

Finally, the density plots of log-transformed ratio features are in Figures 3.8, 3.9, and 3.10. Almost all of these plots for graphs from Section 2.2 (with the exception of the ratio of mean degree) are clearly bimodal with one of the two modes centred around 0. Hence we can infer the existence of two subpopulations: one where pattern and target graphs have very similar properties (the majority for most features) and one where pattern and target graphs are very different. As for the graphs from Section 2.1, the plot of the ratio of the number of vertices in Figure 3.8 is perfectly symmetrical and centred around 0, since the number of vertices is a controlled variable for this database. All of the remaining plots for ratio features have most of the data very close to 0. Thus, the differences between pattern and target graphs are very small. Furthermore, all the distributions are symmetrical—the pattern graph is just as likely to be larger/denser/etc. as the opposite.

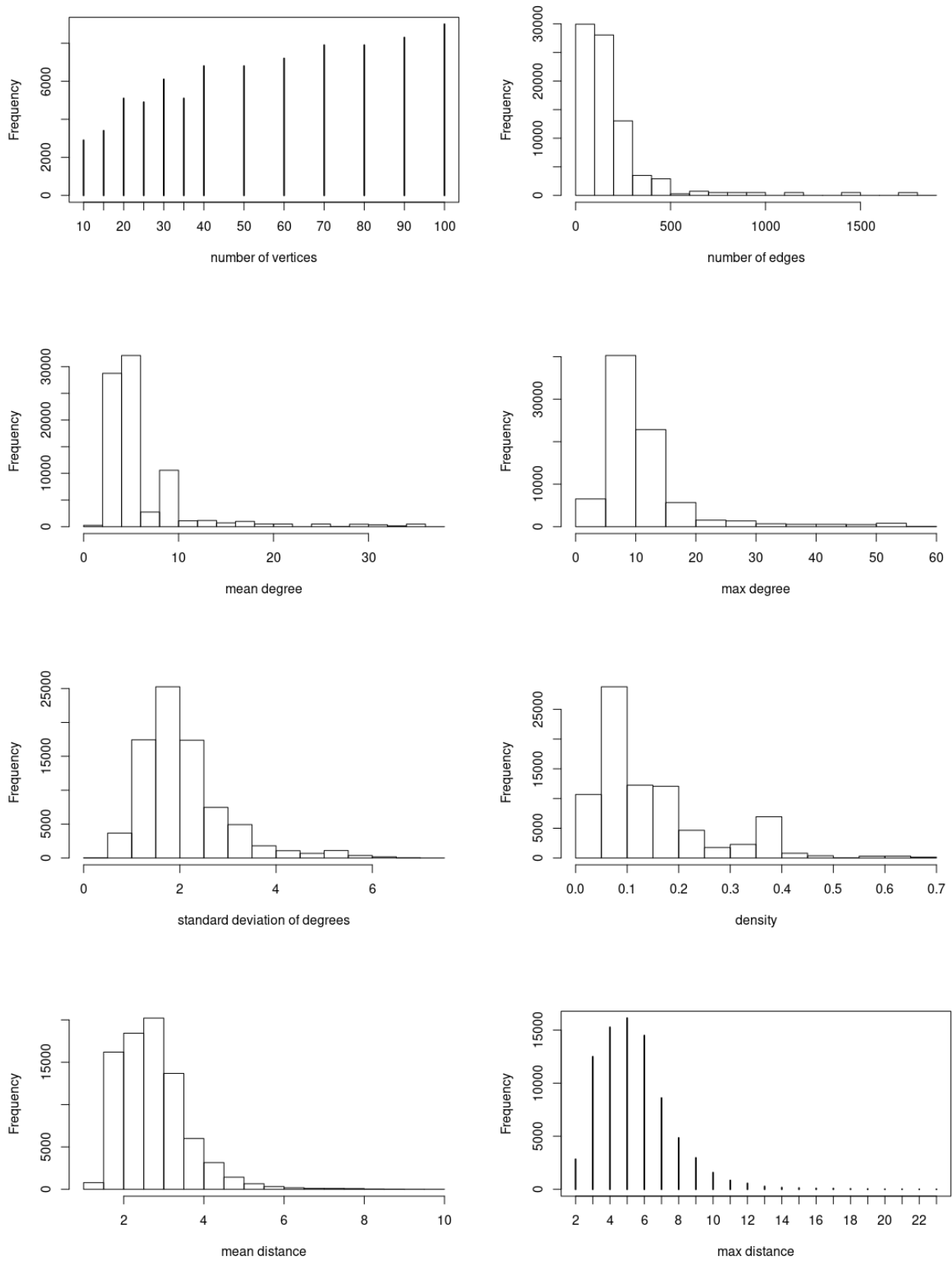


Figure 3.5: Plots of how various features are distributed for graphs from Section 2.1

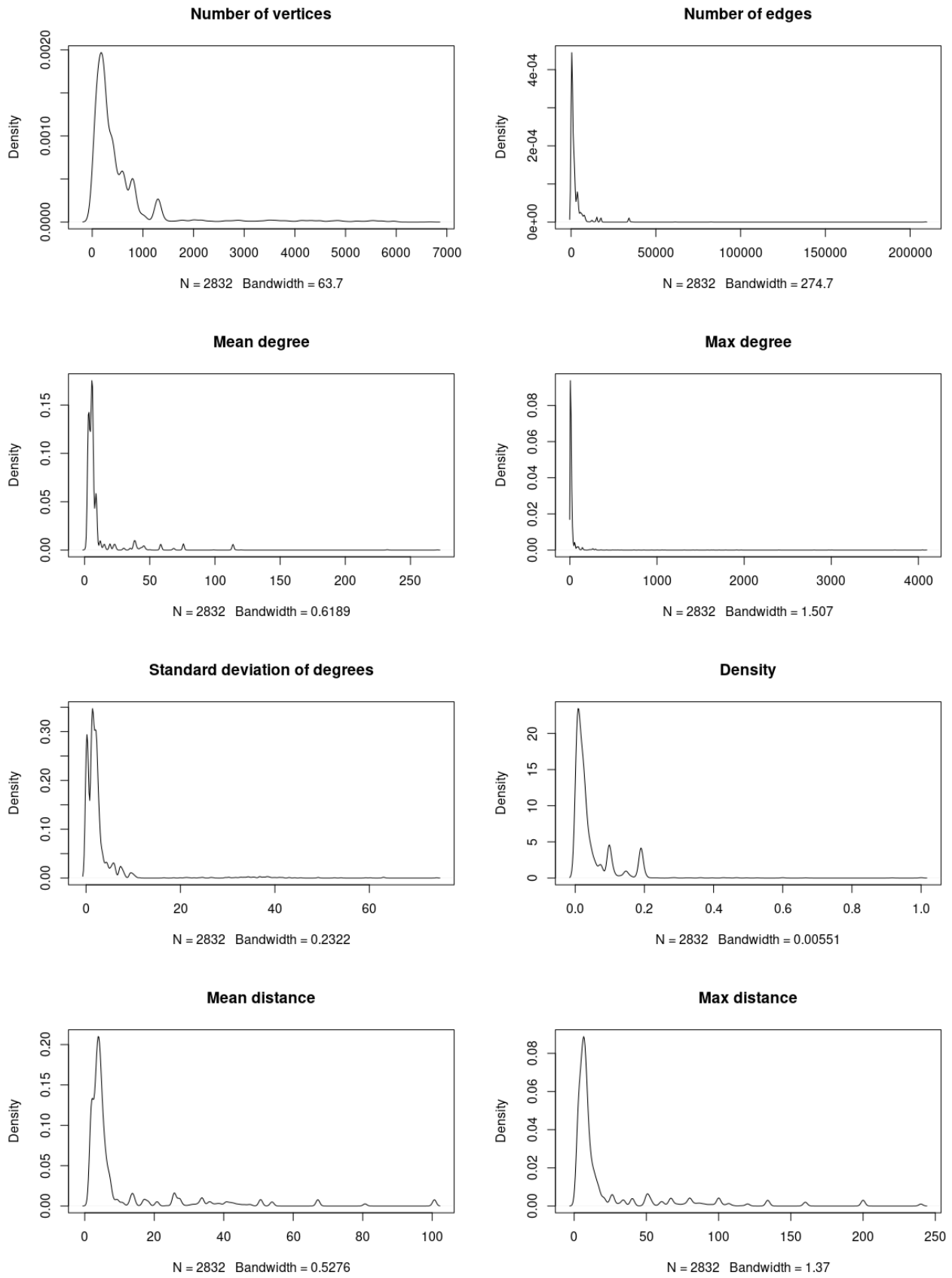


Figure 3.6: Plots of how various features are distributed for graphs from Section 2.2

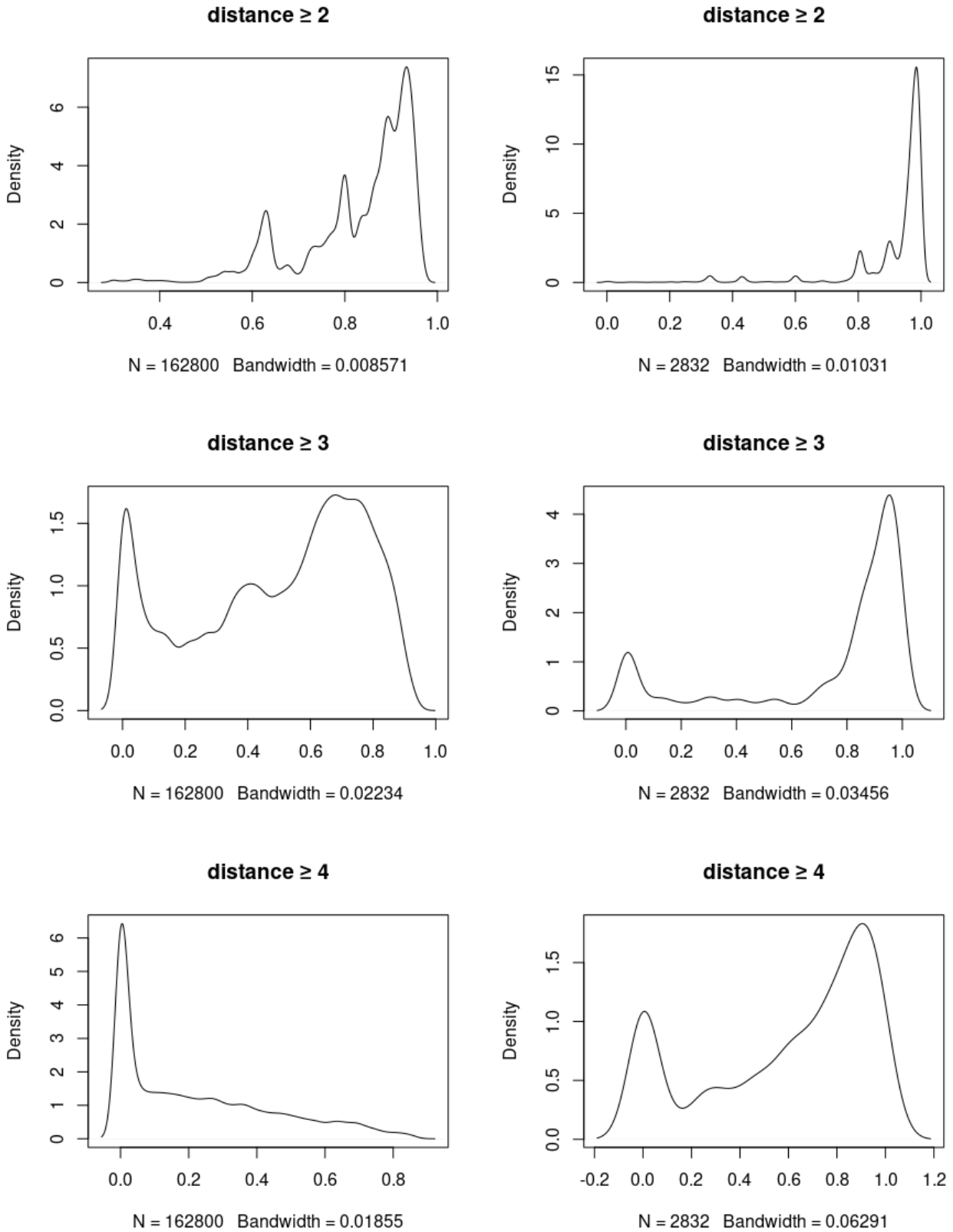


Figure 3.7: Comparison of typical distances between pairs of vertices between the two graph databases with graphs from Section 2.1 on the left and graphs from Section 2.2 on the right

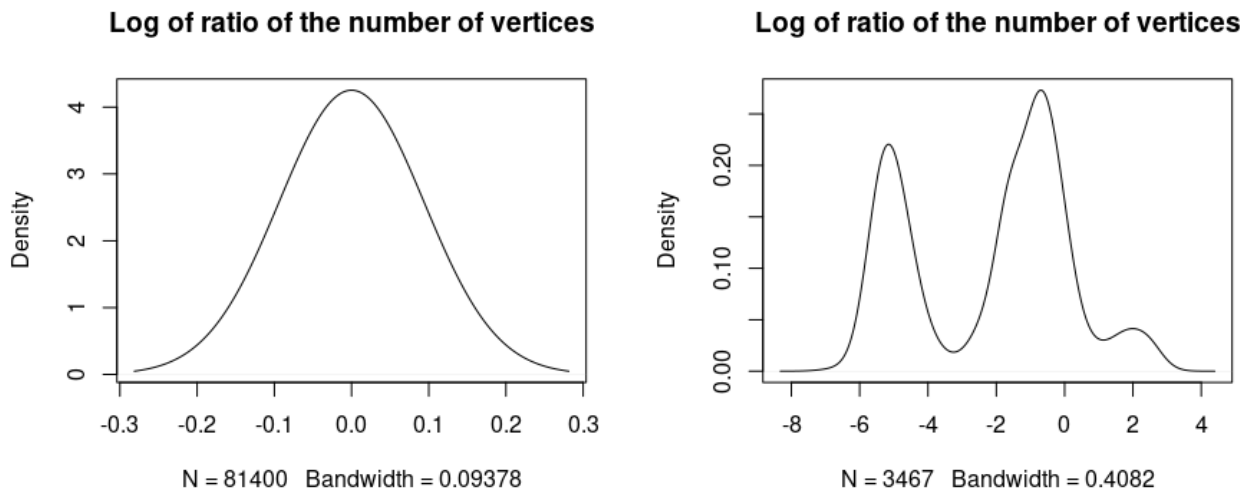


Figure 3.8: The density plots of log-transformed ratio of the number of vertices between pattern and target graphs for both databases with graphs from Section 2.1 on the left and graphs from Section 2.2 on the right

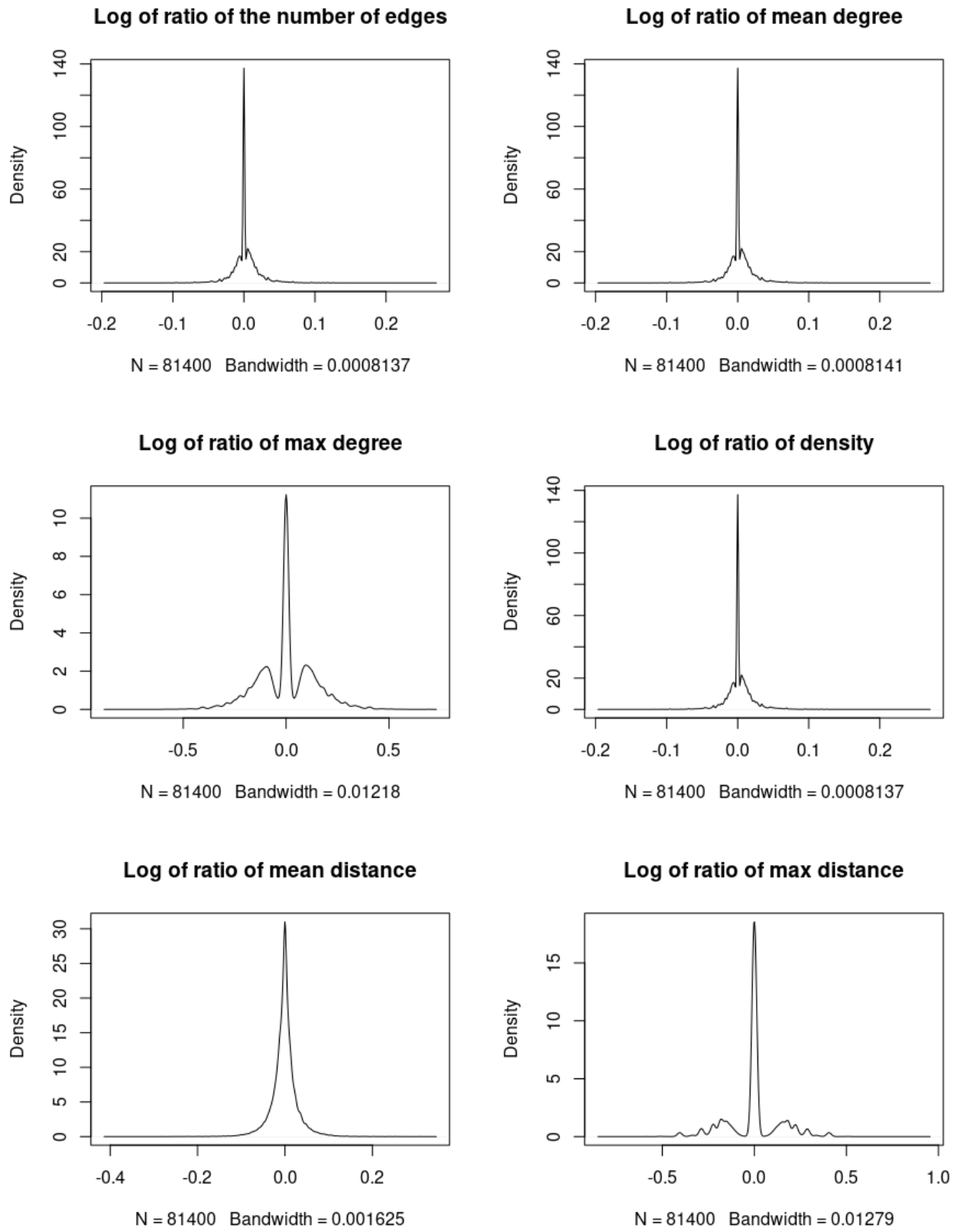


Figure 3.9: The other density plots of the log-transformed ratio features for graphs from Section 2.1

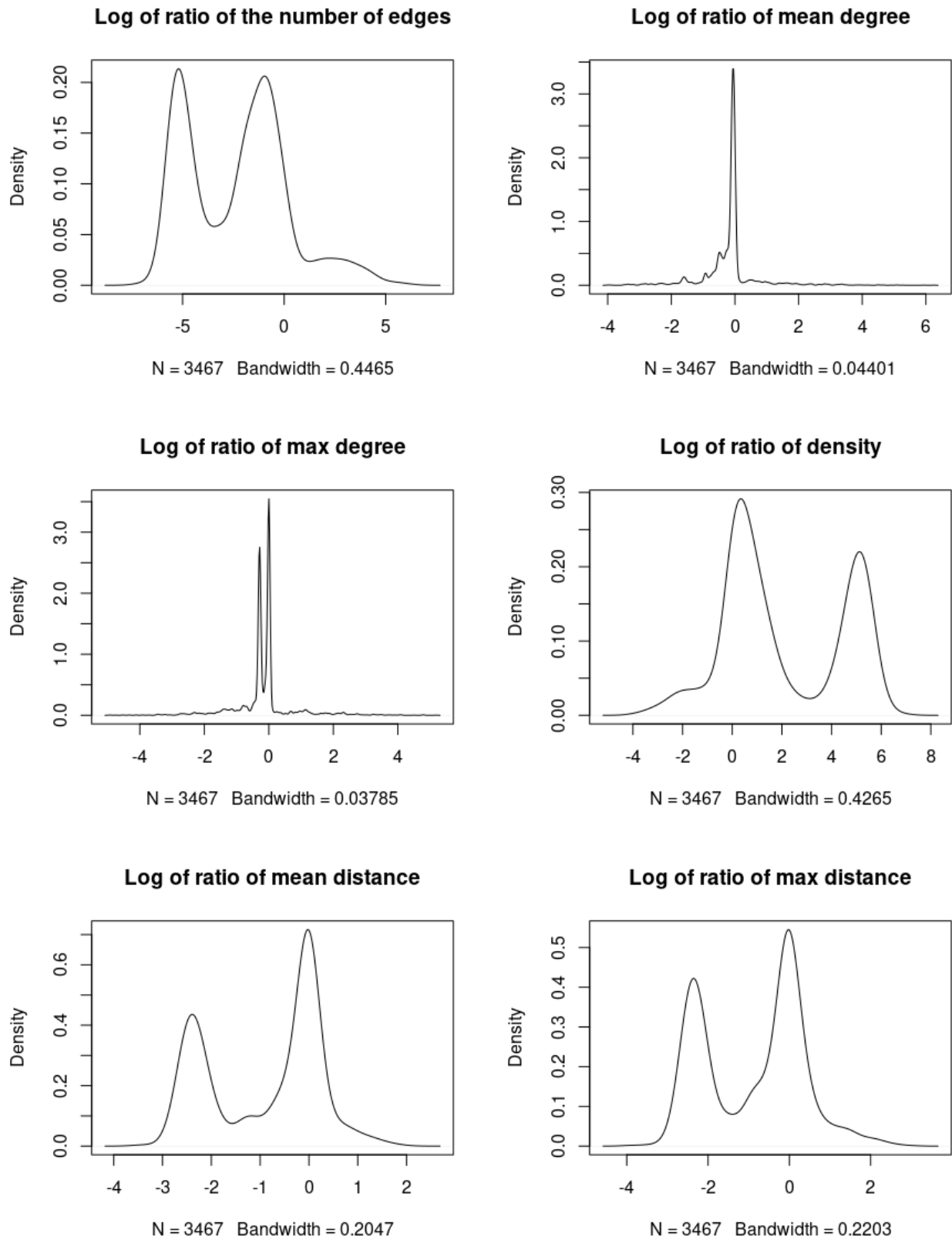


Figure 3.10: The other density plots of the log-transformed ratio features for graphs from Section 2.2

Chapter 4

Machine Learning Models & Their Evaluation

After running the algorithms on all of the data for different types of labelling and p values, an ML algorithm can be trained to predict which algorithm should be chosen for each pair of graphs. For each pair of graphs, LLAMA [13] can take:

- A list of features. With separate features for pattern and target graphs as well as ratio features, we have 33 features in total.
- A list of performance measures for all algorithms, i.e., the values that we are trying to optimise. In this case (as in most cases), this corresponds to running time. The values are capped at the timeout value (1,000,000 ms). Furthermore, instances that were not run on the clique algorithm are also set to the timeout value. Finally, we filter out instances where all of the algorithms timed out.
- A list of boolean values, denoting whether each algorithm successfully finished or not. Timeouts, the clique algorithm running out of memory, and instances that were not run with the clique algorithm because of their size are all marked as false.
- A dataframe, measuring the running time taken to compute each feature for each problem instance, a single number for the approximate time taken to compute all features for any instance, or a list with one or more costs per problem instance. We use the last option with a single cost per instance. This parameter is used to ensure a fair comparison when comparing the portfolio against other algorithms: the runtime of the portfolio is defined as the runtime of its chosen algorithm together with the feature extraction time. While costs for graphs from Section 2.2 reached up to 65 s, the maximum cost for graphs from Section 2.1 is only 6 ms.

After constructing the required dataframes as described above, the data needs to be split into training and test sets. We use a technique called 10-fold *cross-validation*, which splits the data into 10 parts [32]. 9/10^{ths} of the data is used to train the ML algorithm, while the remaining 1/10th is used to evaluate how good the trained model is. This process of training and evaluation is repeated 10 times, letting each of the 10 parts be used for evaluation exactly once. The goodness-of-fit criteria are then averaged out between the 10 runs.

The 10 folds could, of course, be chosen completely randomly. However, research suggests that stratified cross-validation typically outperforms random-sampling-based cross-validation and results in a better model [11]. Suppose we have a dataset of N elements. *Stratified sampling* partitions it into a number of subpopulations s_1, \dots, s_n with n_1, \dots, n_N elements respectively (typically based on the value of some feature or collection of

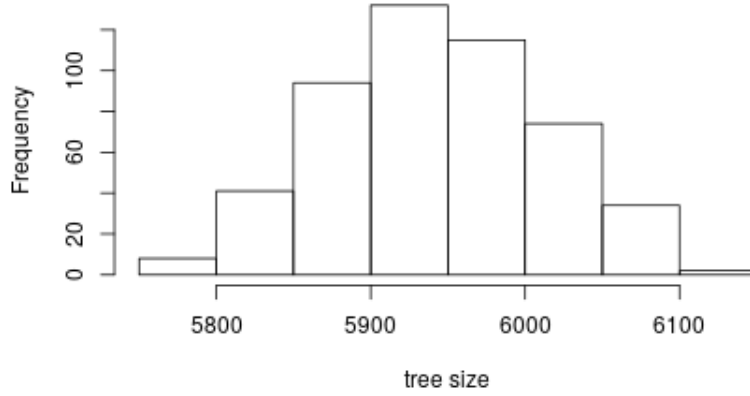


Figure 4.1: A histogram of the number of nodes in each tree

features). It then draws from each subpopulation independently, ensuring that approximately n_i/N of the sample comes from subpopulation s_i for $i = 1, \dots, n$ [19]. In this case the data is partitioned into four groups based on which algorithm performed best.

The cross-validation folds are then passed to the ML algorithm. LLAMA [12, 13] supports algorithm portfolios based on three different types of ML algorithms:

Classification The ML algorithm predicts which algorithm is likely to perform best on each problem instance.

Regression Each algorithm’s data is used to train a separate ML model, predicting the algorithm’s performance. The winning algorithm can then be chosen based on those predictions.

Clustering All instances of the training data are clustered and the best algorithm is determined for each cluster. New problem instances can then be assigned to the nearest cluster.

We are using a classification algorithm called random forests [3] and its implementation in R [17]. We chose this algorithm as it is recommended in the LLAMA manual [12] and successfully used in a similar study [15]. We use the default number of trees (500), and the number of nodes per tree is plotted in Figure 4.1.

In order to discuss and analyse the ML algorithm in more detail, we introduce some new terminology. Each problem instance with features and running times in the training dataset is called an *observation*. The *class* of an observation is the algorithm with lowest running time for that problem instance. Previously discussed features of graphs are sometimes referred to as (*independent*) *variables*. The (*problem*) *instance space* is the Cartesian product of the domains of features [28], where a *domain* of X (denoted $\text{dom } X$) is a set of all possible values that X can take.

A (*classification*) *decision tree* is “a classifier expressed as a recursive partition of the instance space” [28]. Typically, it can be represented as a rooted binary tree, where each internal node *splits* the instance space into two regions based on the value of one of the features. For example, for some feature X and a particular value $x \in \text{dom } X$, the left child might be assigned all observations with $X < x$, while the right child would get observations with $X \geq x$. For each leaf node, we can count how many of its observations belong to each class and assign the most highly represented class to that node.

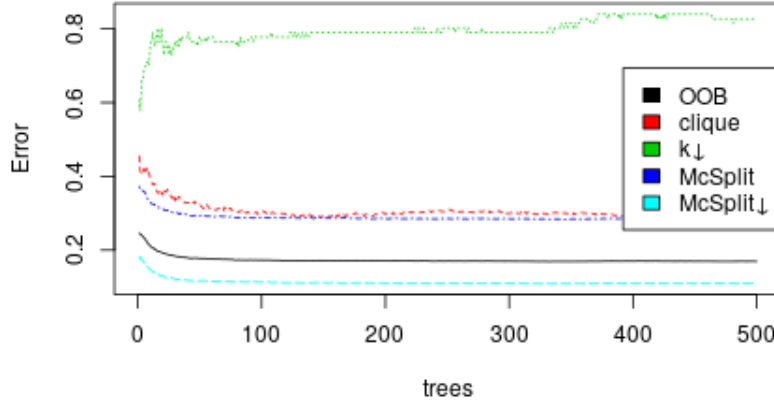


Figure 4.2: Convergence plot of various error measures as the number of trees in a random forest increases. The plot shows the OOB error and $1 - \text{recall}$ for each algorithm.

Remark 4.0.1. Other possibilities include a node having more than two children and a split being made in a more complicated way. Although trees with such properties fit the definition of a decision tree, standard machine learning algorithms are more restrictive [10, 28].

When a decision tree is used to make a classification prediction, a data point travels from node to node (starting at the root node) according to the splitting rules. When it reaches a leaf node, the class assigned to that node is outputted as the tree’s prediction.

A *random forest* builds a collection of decision trees [10]. Suppose we have p variables. Then each time a split is considered, the variable to split on is chosen from \sqrt{p} rather than p variables. Therefore, the strongest predictors are sometimes not even considered, ensuring a level of diversity among the trees. An individual tree’s prediction is called a *vote*. A classifying random forest predicts by collecting the votes from all of the trees and predicting the class with the highest number of votes.

Lastly, we used the `parallelMap` package to train the model using multiple threads. Furthermore, the R code was heavily optimised to remove temporary variables as soon as they are no longer needed in order to reduce memory consumption.

4.1 Unlabelled Graphs

4.1.1 Error Rates

Random forests support a convenient way to estimate the test error without cross-validation or any other kind of data splitting. Each tree in a random forest uses around $2/3$ of the data [10]. The remaining $1/3$ is referred to as *out-of-bag* (OOB) observations. For each observation in the data, we can predict the answer (the vote on which algorithm is expected to win) using all trees that have the observation as OOB. The majority vote is then declared to be the answer. The *OOB error* is the relative frequency of incorrect predictions [10]. As each prediction was made using trees that had not seen that particular observation before, OOB error is a valid estimate of test error. The black line in Figure 4.2 shows how the error converges with the number of trees to about 17%.

The other lines in the figure, one for each algorithm, are defined as $1 - \text{recall}$, where, for an algorithm A , *recall* [25] is

$$\frac{\text{the number of instances that were correctly predicted as } A}{\text{the number of instances where } A \text{ is the correct prediction}}.$$

The error rates for MCSPLIT \downarrow , MCSPLIT, the clique encoding, and $k \downarrow$ converge to 11%, 29%, 30%, and 80% respectively. Unlike the errors of all the other classes, the error of $k \downarrow$ has an upward trend and converges to a very high value. Perhaps the model eventually learns not to predict $k \downarrow$ very often and the data points with $k \downarrow$ winning are treated as randomness in the data more so than a statistically significant trend.

4.1.2 Variable Importance

Next we are going to explore how important each feature is in making predictions, but for that we need to introduce some new definitions. Consider a single tree T in a random forest. The root of T can be reached by any observation, regardless of the values of its features. After passing some node n , some feature is restricted, i.e., it is imposed an upper or lower limit on the kind of values it can have for it to move towards a particular child of n . The part of feature space that an observation can have while at some node n is called a *region*.

Definition 4.1.1. Suppose we have K classes. Consider some region m . The *Gini index* is then defined as

$$G = \sum_{k=1}^K \hat{p}_{mk}(1 - \hat{p}_{mk}),$$

where \hat{p}_{mk} represents the proportion of observations in region m that are from class k (i.e., have algorithm k as the best algorithm) [10].

As we move down a tree, we want the region to be restricted to a single class. Then the observations from the training data that satisfy the conditions imposed by the parent nodes would be classified with perfect accuracy. The Gini index is at its lowest when all the proportions \hat{p}_{mk} are close to either 0 or 1, meaning that almost all the observations in the region belong to a single class. Hence the Gini index is often used to evaluate the quality of a split.

Remark 4.1.1. Note that $G = 0$ when any single $\hat{p}_{mk} = 0$, regardless of the values of other proportions. Therefore $G = 0$ does not automatically imply that the tree is a good classifier.

The variable importance measure of feature f in Figure 4.3 is calculated as the amount by which the Gini index decreases after passing nodes that use feature f , averaged over all trees in the random forest [10]. Looking at the figure more closely, the standard deviations of degrees of both target and pattern graphs are by far the most important predictors. Unsurprisingly, the worst predictors are the features with very low variance: number of loops and connectedness of both graphs. Perhaps more surprisingly, the ratio features are not as successful as one might have hoped: the ratio of the numbers of vertices is at the bottom 5th place and the best ratio feature, the mean distance ratio, is only 10th. Last thing to note is that features of the pattern graph are always behind the same features of the target graph and usually not far behind. Perhaps this is due to some datasets having less pattern graphs, or pattern graphs having fewer vertices. The variable usage plot in Figure 4.4 tells a similar story: the orders are not identical, but there are no big outliers.

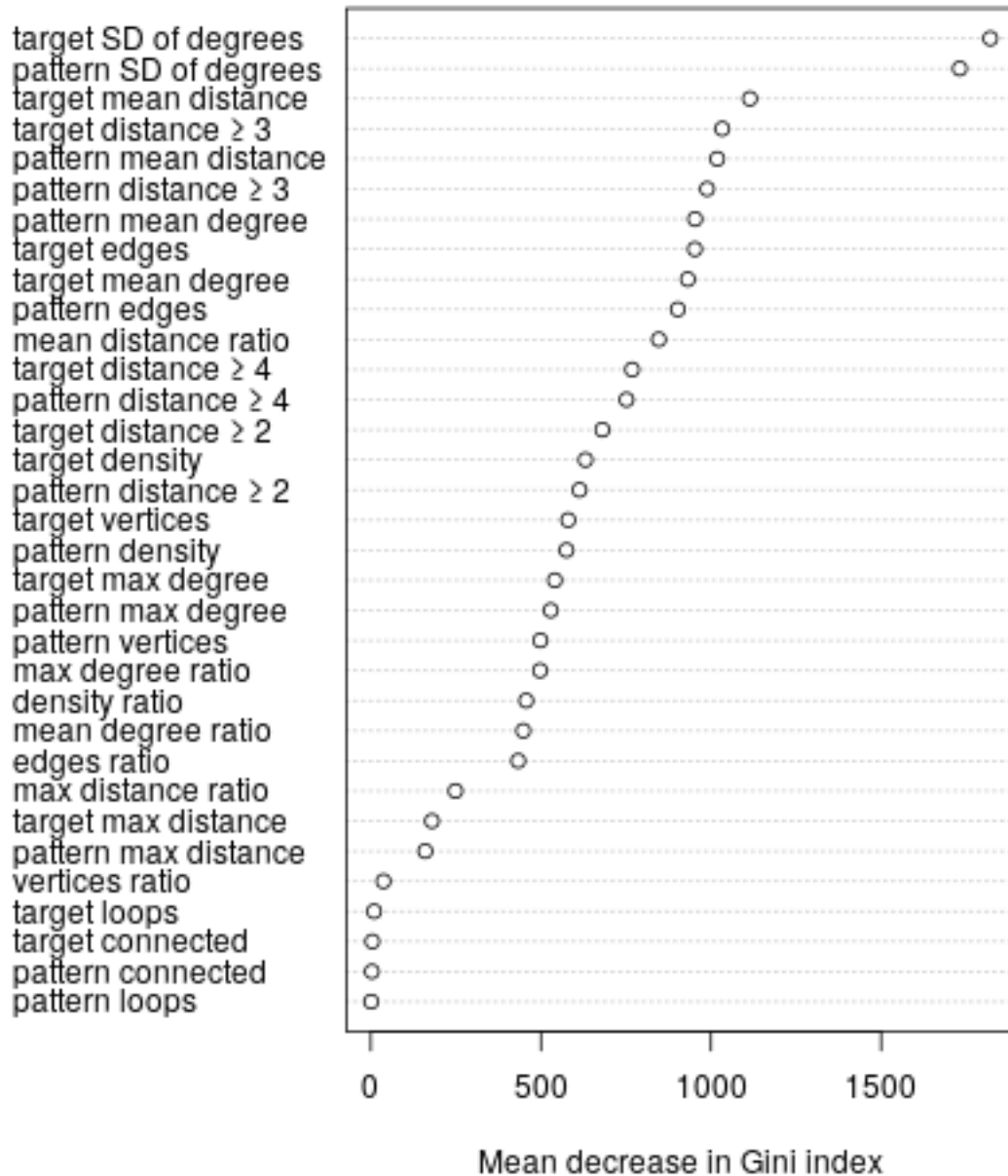


Figure 4.3: Dotchart of variable importance calculated based on the Gini index and sorted from most important to least important

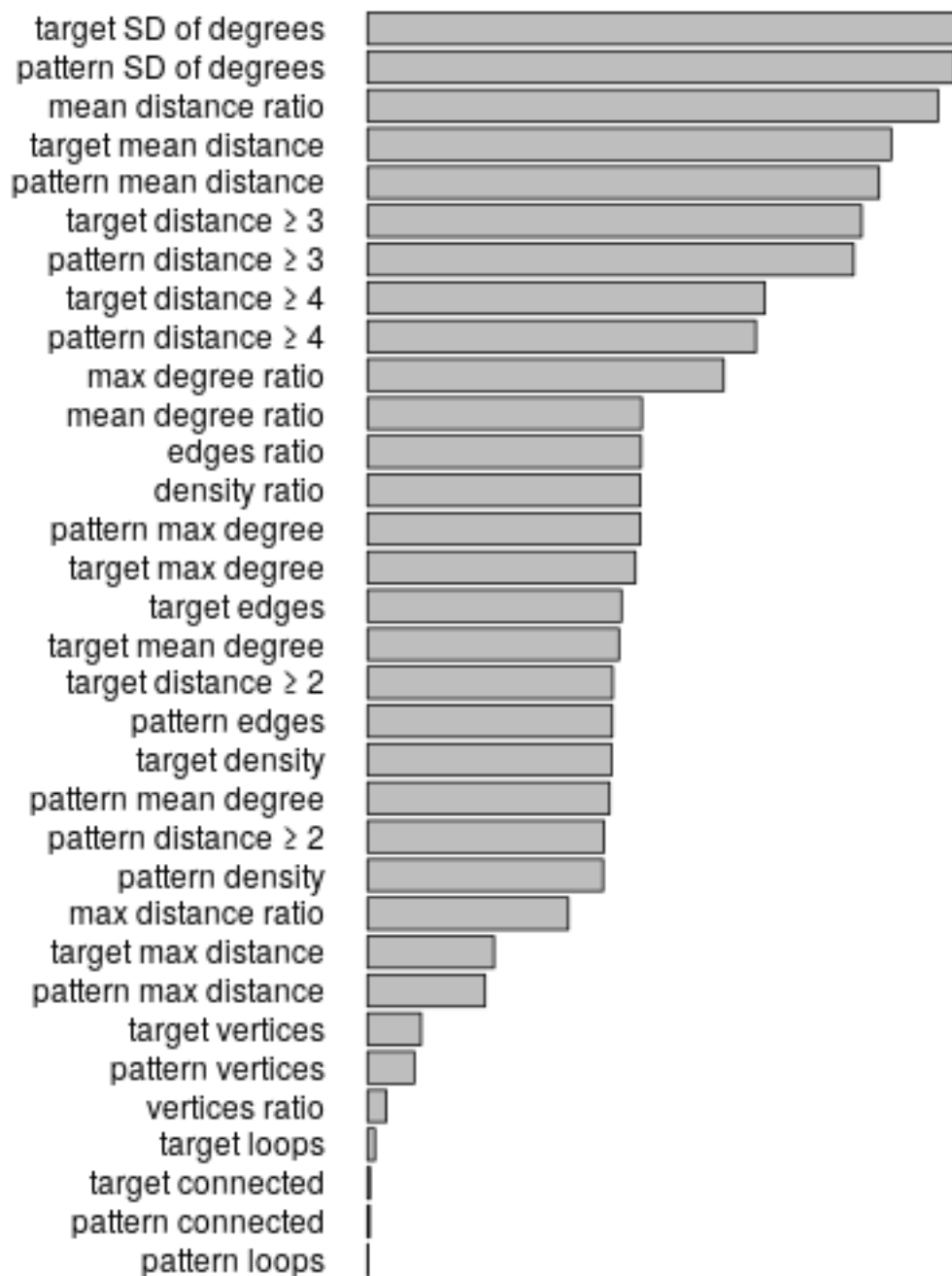


Figure 4.4: How often was each variable used to make splitting decisions?

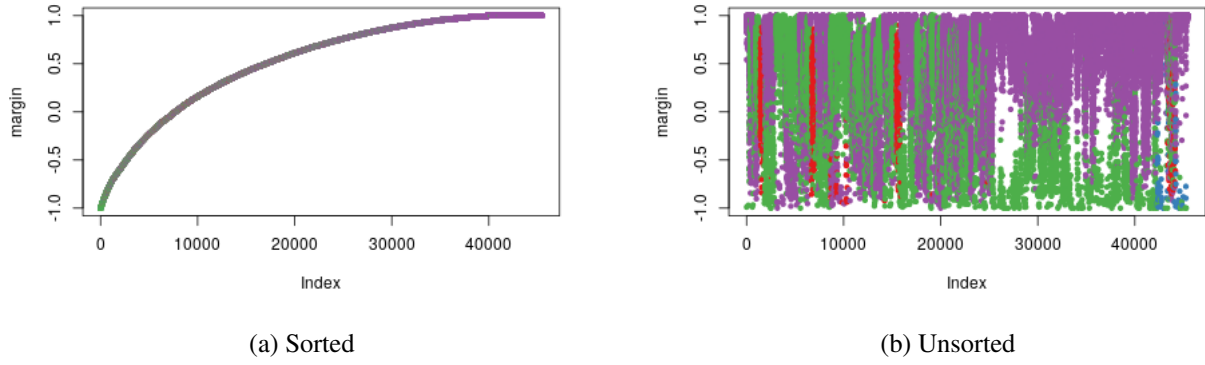


Figure 4.5: Margins of all the data points. MCSPLIT is in green, MCSPLIT ↓ is in purple, $k \downarrow$ is in blue, and the clique encoding is in red.

4.1.3 Margins

Definition 4.1.2. Let c_1, \dots, c_n be n classes and let p be a data point that belongs to class c_p . Let v_1, \dots, v_n denote the number of votes for each class when given p as input. The *margin* of p is

$$\frac{v_p}{\sum_{i=1}^n v_i} - \max_{i \neq p} \frac{v_i}{\sum_{j=1}^n v_j},$$

which is a number in $[-1, 1]$ [18].

A value above 0 means that the forest as a whole predicted correctly. A margin of 1 would mean that all trees voted correctly. Figure 4.5 shows the sorted and unsorted margin of all data points. We can recognise the same error rates as in Figure 4.2 as well as areas where MCSPLIT and MCSPLIT ↓ dominate. We also plot the histograms of how the margins are distributed for each algorithm in Figure 4.6. We note that:

- Instances best handled by the clique encoding are usually recognised, but with significant uncertainty.
- We are usually wrong about $k \downarrow$ (probably because it is a winning algorithm in only 0.44% of all cases).
- When faced with an instance that is best handled by MCSPLIT ↓, the vast majority of the trees vote correctly.
- MCSPLIT detection rates are decent, but far behind those of MCSPLIT ↓.

4.1.4 Partial Dependence

Since the standard deviations of degrees in both target and pattern graphs are the most important features, we plot partial dependence plots for the standard deviation of degrees in the target graph for MCSPLIT ↓ and the clique encoding in Figure 4.7. The plotted function [18] is defined as

$$f(x) = \log p_k(x) - \frac{1}{K} \sum_{i=1}^K \log p_i(x),$$

where:

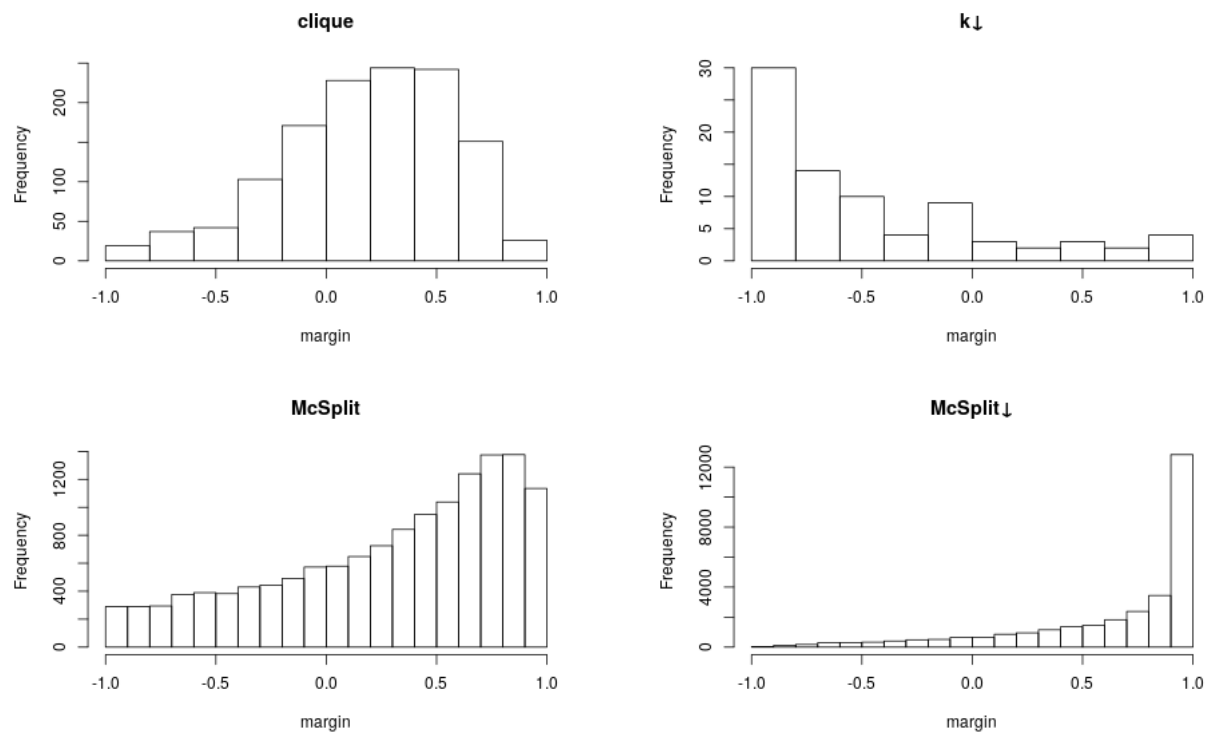


Figure 4.6: Histograms of margins for each winning algorithm

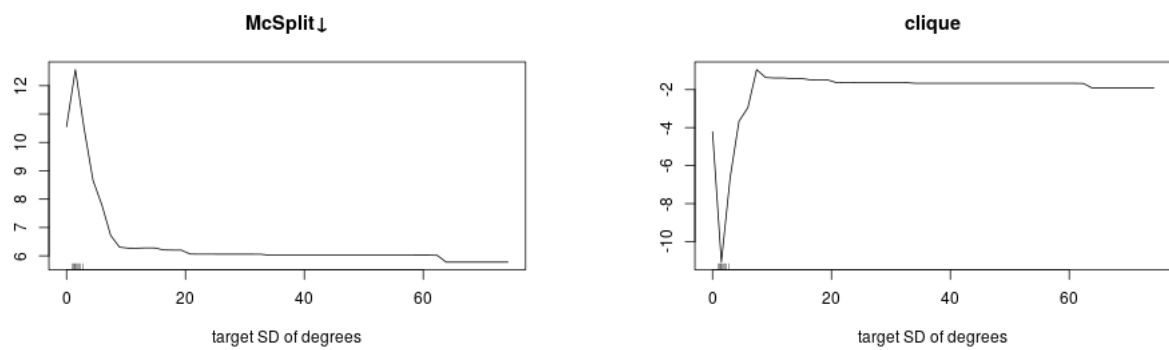


Figure 4.7: Partial dependence plots for the standard deviation of degrees of the target graph

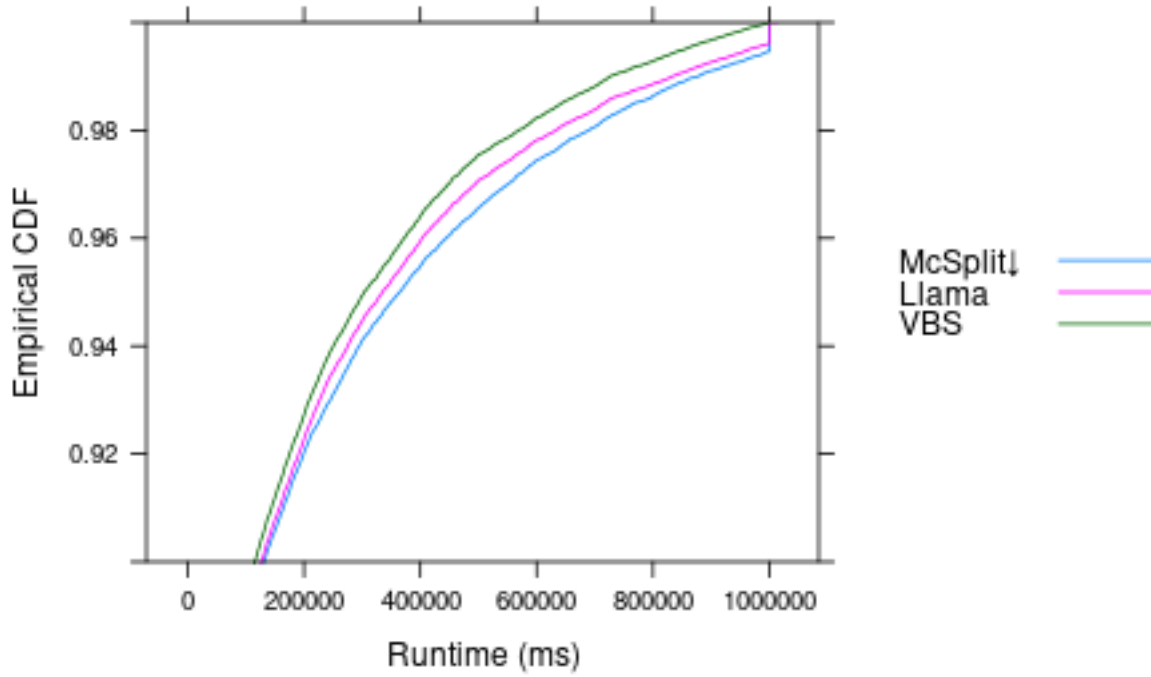


Figure 4.8: LLAMA model compared to the VBS and MCSPLIT ↓

- x is the value on the horizontal axis (in this case standard deviation of degrees in the target graph),
- $p_i(x)$ is the proportion of votes for class i for a problem instance with a standard deviation of degrees in the target graph equal to x ,
- K is the number of classes,
- and k is the main class under consideration (MCSPLIT ↓ and the clique encoding).

Essentially, $f(x)$ compares the proportion of votes for class k with the average value over all classes. We can deduce that a low standard deviation of degrees is a strong sign that MCSPLIT and MCSPLIT ↓ should perform well. On the other hand, the clique encoding is expected to perform better on graphs with high variance of degrees. However, $\max f(x)$ for the clique encoding is just barely above 0 and much lower than $\min f(x)$ for MCSPLIT ↓, meaning that the standard deviation of degrees does not provide enough information to choose the clique encoding over MCSPLIT or MCSPLIT ↓.

Remark 4.1.2. We omit the plots for the other two algorithms as the plot for MCSPLIT looks the same as the one for MCSPLIT ↓ and prediction success rate for k ↓ is so low that a plot for k ↓ would be meaningless.

Remark 4.1.3. The plots for the standard deviation of degrees of the pattern graph are omitted since they are identical to those of the target graph.

4.1.5 Runtime Comparison

In order to compare the LLAMA model with other algorithms, we treat the VBS as the upper bound and the single best solver MCSPLIT ↓ as the lower bound. Out of 45468 instances solved by at least one algorithm, our model managed to solve 45290, compared to 45223 solved by MCSPLIT ↓. In other words, it was able to close 27.3% of the gap between our lower and upper bounds in terms of instances solved within the time limit. Figure 4.8

shows how the ML model compares to the VBS and the single best solver MCSPLIT ↓ (note that the vertical axis starts at 0.9 rather than 0). Unsurprisingly, the model outperforms MCSPLIT ↓, but does not reach the best possible performance represented by the VBS.

4.2 Vertex-Labelled Graphs

4.3 Vertex- and Edge-Labelled Graphs

Bibliography

- [1] Zeina Abu-Aisheh. *Anytime and Distributed Approaches for Graph Matching*. PhD thesis, Université François-Rabelais de Tours, 2016.
- [2] Bernd Bischl, Pascal Kerschke, Lars Kotthoff, Marius Thomas Lindauer, Yuri Malitsky, Alexandre Fréchette, Holger H. Hoos, Frank Hutter, Kevin Leyton-Brown, Kevin Tierney, and Joaquin Vanschoren. Aslib: A benchmark library for algorithm selection. *Artif. Intell.*, 237:41–58, 2016.
- [3] Leo Breiman. Random forests. *Machine Learning*, 45(1):5–32, 2001.
- [4] Stephen A. Cook. The complexity of theorem-proving procedures. In Michael A. Harrison, Ranan B. Banerji, and Jeffrey D. Ullman, editors, *Proceedings of the 3rd Annual ACM Symposium on Theory of Computing, May 3-5, 1971, Shaker Heights, Ohio, USA*, pages 151–158. ACM, 1971.
- [5] Guillaume Damiand, Christine Solnon, Colin de la Higuera, Jean-Christophe Janodet, and Émilie Samuel. Polynomial algorithms for subisomorphism of nd open combinatorial maps. *Computer Vision and Image Understanding*, 115(7):996–1010, 2011.
- [6] Reinhard Diestel. *Graph Theory, 5th Edition*, volume 173 of *Graduate texts in mathematics*. Springer-Verlag, 2016.
- [7] Hans-Christian Ehrlich and Matthias Rarey. Maximum common subgraph isomorphism algorithms and their applications in molecular science: a review. *Wiley Interdisciplinary Reviews: Computational Molecular Science*, 1(1):68–79, 2011.
- [8] Pasquale Foggia, Carlo Sansone, and Mario Vento. A database of graphs for isomorphism and sub-graph isomorphism benchmarking. In *Proceedings of the 3rd IAPR TC-15 International Workshop on Graph-based Representations*, 2001.
- [9] Ruth Hoffmann, Ciaran McCreesh, and Craig Reilly. Between subgraph isomorphism and maximum common subgraph. In Satinder P. Singh and Shaul Markovitch, editors, *Proceedings of the Thirty-First AAAI Conference on Artificial Intelligence, February 4-9, 2017, San Francisco, California, USA.*, pages 3907–3914. AAAI Press, 2017.
- [10] Gareth James, Daniela Witten, Trevor Hastie, and Robert Tibshirani. *An Introduction to Statistical Learning: With Applications in R*. Springer Publishing Company, Incorporated, 2014.
- [11] Ron Kohavi. A study of cross-validation and bootstrap for accuracy estimation and model selection. In *Proceedings of the Fourteenth International Joint Conference on Artificial Intelligence, IJCAI 95, Montréal Québec, Canada, August 20-25 1995, 2 Volumes*, pages 1137–1145. Morgan Kaufmann, 1995.
- [12] Lars Kotthoff. LLAMA: leveraging learning to automatically manage algorithms. Technical Report arXiv:1306.1031, arXiv, June 2013.
- [13] Lars Kotthoff, Bernd Bischl, Barry Hurley, and Talal Rahwan. *Leveraging Learning to Automatically Manage Algorithms*. CRAN, December 2015.

- [14] Lars Kotthoff, Pascal Kerschke, Holger Hoos, and Heike Trautmann. Improving the state of the art in inexact TSP solving using per-instance algorithm selection. In Clarisse Dhaenens, Laetitia Jourdan, and Marie-Éléonore Marmion, editors, *Learning and Intelligent Optimization - 9th International Conference, LION 9, Lille, France, January 12-15, 2015. Revised Selected Papers*, volume 8994 of *Lecture Notes in Computer Science*, pages 202–217. Springer, 2015.
- [15] Lars Kotthoff, Ciaran McCreesh, and Christine Solnon. Portfolios of subgraph isomorphism algorithms. In Paola Festa, Meinolf Sellmann, and Joaquin Vanschoren, editors, *Learning and Intelligent Optimization - 10th International Conference, LION 10, Ischia, Italy, May 29 - June 1, 2016, Revised Selected Papers*, volume 10079 of *Lecture Notes in Computer Science*, pages 107–122. Springer, 2016.
- [16] Giorgio Levi. A note on the derivation of maximal common subgraphs of two directed or undirected graphs. *CALCOLO*, 9(4):341, Dec 1973.
- [17] Andy Liaw and Matthew Wiener. Classification and regression by randomforest. *R News*, 2(3):18–22, 2002.
- [18] Andy Liaw and Matthew Wiener. *Breiman and Cutler’s Random Forests for Classification and Regression*. CRAN, October 2015.
- [19] Sharon L. Lohr. *Sampling: Design and Analysis*. Advanced (Cengage Learning). Cengage Learning, 2009.
- [20] Ciaran McCreesh, Samba Ndoj Ndiaye, Patrick Prosser, and Christine Solnon. Clique and constraint models for maximum common (connected) subgraph problems. In Michel Rueher, editor, *Principles and Practice of Constraint Programming - 22nd International Conference, CP 2016, Toulouse, France, September 5-9, 2016, Proceedings*, volume 9892 of *Lecture Notes in Computer Science*, pages 350–368. Springer, 2016.
- [21] Ciaran McCreesh and Patrick Prosser. The shape of the search tree for the maximum clique problem and the implications for parallel branch and bound. *TOPC*, 2(1):8:1–8:27, 2015.
- [22] Ciaran McCreesh, Patrick Prosser, and James Trimble. Heuristics and really hard instances for subgraph isomorphism problems. In Subbarao Kambhampati, editor, *Proceedings of the Twenty-Fifth International Joint Conference on Artificial Intelligence, IJCAI 2016, New York, NY, USA, 9-15 July 2016*, pages 631–638. IJCAI/AAAI Press, 2016.
- [23] Ciaran McCreesh, Patrick Prosser, and James Trimble. A partitioning algorithm for maximum common subgraph problems. In Carles Sierra, editor, *Proceedings of the Twenty-Sixth International Joint Conference on Artificial Intelligence, IJCAI 2017, Melbourne, Australia, August 19-25, 2017*, pages 712–719. ijcai.org, 2017.
- [24] Panos M. Pardalos and Jue Xue. The maximum clique problem. *J. Global Optimization*, 4(3):301–328, 1994.
- [25] David M. W. Powers. Evaluation: from precision, recall and f-measure to roc, informedness, markedness and correlation. *Journal of Machine Learning Technologies*, 2(1):37–63, 2011.
- [26] John W. Raymond and Peter Willett. Maximum common subgraph isomorphism algorithms for the matching of chemical structures. *Journal of Computer-Aided Molecular Design*, 16(7):521–533, 2002.
- [27] John R. Rice. The algorithm selection problem. *Advances in Computers*, 15:65–118, 1976.
- [28] Lior Rokach and Oded Maimon. *Data Mining with Decision Trees - Theory and Applications*. 2nd Edition, volume 81 of *Series in Machine Perception and Artificial Intelligence*. WorldScientific, 2014.
- [29] Massimo De Santo, Pasquale Foggia, Carlo Sansone, and Mario Vento. A large database of graphs and its use for benchmarking graph isomorphism algorithms. *Pattern Recognition Letters*, 24(8):1067–1079, 2003.

- [30] Christine Solnon. Alldifferent-based filtering for subgraph isomorphism. *Artif. Intell.*, 174(12-13):850–864, 2010.
- [31] Christine Solnon, Guillaume Damiand, Colin de la Higuera, and Jean-Christophe Janodet. On the complexity of submap isomorphism and maximum common submap problems. *Pattern Recognition*, 48(2):302–316, 2015.
- [32] Andrew R. Webb. *Statistical Pattern Recognition, 2nd Edition*. John Wiley & Sons, October 2002.
- [33] Eric W. Weisstein. k-subset. *MathWorld – A Wolfram Web Resource*, April 2004.
- [34] Martin B. Wilk and Ramanathan Gnanadesikan. Probability plotting methods for the analysis of data. *Biometrika*, 55(1):1–17, 1968.
- [35] Stéphane Zampelli, Yves Deville, and Christine Solnon. Solving subgraph isomorphism problems with constraint programming. *Constraints*, 15(3):327–353, 2010.